

Evaluation of the Impact of Thresholding and Frequency/Time Resolution on Signal Area Estimation Methods

Mohammed M. Alammar

*Department of Electrical Engineering and Electronics
University of Liverpool
Liverpool, United Kingdom
King Khalid University, Abha, Saudi Arabia
M.M.Alammar@liverpool.ac.uk*

Miguel López-Benítez

*Department of Electrical Engineering and Electronics
University of Liverpool
Liverpool, United Kingdom
ARIES Research Centre, Antonio de Nebrija University, Spain
M.Lopez-Benitez@liverpool.ac.uk*

Abstract—Spectrum awareness is an essential aspect of wireless communication technology. Wireless communication systems can obtain spectrum awareness information by monitoring the spectrum usage in the frequency and time domains and representing this information as a time-frequency matrix. In many practical cases it is useful to determine the subsets of elements of such matrix where a signal is present (i.e., the signal area). Several signal area (SA) estimation methods with varying performance have been proposed in the literature. However, there is a lack of comparative research that shows how the configuration of such methods affects their relative performance. In this context, this work investigates the impact of two essential configuration aspects for any SA method, namely the threshold used to decide whether each element of the time/frequency grid contains a signal component or just noise, and the frequency/time resolution of the measurements carried out to obtain such data matrix. Several popular threshold decision criteria and a broad range of measurement resolutions are investigated, showing that these two particular aspects play a key role in the optimum configuration and performance of SA estimation methods. Several useful findings and design guidelines are provided as well.

Index Terms—Spectrum awareness, signal area estimation, signal detection

I. INTRODUCTION

Wireless communication relies on spectrum awareness systems (SAS) to allocate spectrum to users. The introduction of dynamic spectrum access (DSA) has helped secondary users (SU) be assigned the spectrum without interfering with the primary users (PU). Besides, the utilized spectrum by paid users leave significant white space (WS), which can be assigned to secondary users [1]. According to [2], it is necessary to have spectrum usage detection methods that can attain high accuracy, low cost, and low latency, to achieve the smart spectrum assignment to SU. Spectrum usage detection can be useful in other application scenarios such as compliance verification and enforcement of spectrum regulations as well as network planning and optimization. Thus, there is a need to implement techniques that ensure high performance in SAS.

Signal Area (SA) estimation is an essential process in SAS and it entails determining the subsets of elements of a time-

frequency matrix where a signal is present (i.e., the signal area). Several SA estimation methods with varying performance have been proposed in the literature. According to [3], spectrum usage detection processes include Fast Fourier transform (FFT), Energy detection (ED), and the SA estimation. Since FFT and ED have been researched in [4] and the best methods proposed, the focus of this research shall be on SA estimation. Research done by [2] shows that the application of SA estimation methods has enabled the reduction of cost and attainment of high accuracy. However, the challenges affecting the techniques include practical limitations and inaccuracies such as false alarms and missed detection [3]. This research shall concentrate on a comparative study of the performance of SA methods under different configuration parameters because several SA estimation methods with varying performance have been proposed but there is a lack of comparative research to show how the configuration of such methods affects their relative performance.

SA can be detected based on several methods. The methods include ED techniques such as the Fourier transform energy detection or the simple signal area estimation (SSA) algorithm described in [2], [3], [5]. Besides, the contour tracing SA (CT-SA) estimation algorithm [6] can be applied. The three methods have been proposed in previous studies [7]. However, there is no comparative study to evaluate the performance of the three methods under different configuration parameters. Such a comparative study would aid in establishing the most appropriate SA estimation method and provide useful insights into the optimum design and configuration of SA estimation methods in practical deployments.

Configuration parameters that have been proposed in previous studies include varying the threshold for energy decisions and the frequency/time resolution of spectrum measurements [2], [8]. Threshold selection is affected by calculations such as the Time of Arrival (TOA) and the signal to noise ratio (SNR). Besides, a study in [7] has proposed a method of a threshold estimation technique that accounts for SNR, intending to adapt a normalized threshold [9]. However, frequency/time resolu-

tion depends on other parameters that shall be discussed in this research. Thus, this study entails an evaluation of the impact of these parameters and their corresponding significance in SA estimation techniques. The main contributions of this study include:

- A comparative study on the three main methods of SA estimation that have been proposed in the literature, including ED, CT-SA and SSA.
- Evaluation of the impact of the threshold selection method on the performance of SA methods under various operational parameters.
- Evaluation of the impact of frequency/time resolution on the estimated SA under various operational parameters.
- Establishment of the most appropriate configuration for SA estimation methods and gaining of some useful insights into the optimum design and configuration of SA estimation methods.

The rest of this paper is organised as follows. First, Section II provides a formal description of the SA estimation problem considered in this work and an overview of the main SA estimation methods proposed to the date. Section III describes the methodology employed in this work to assess and compare the performance of the considered SA estimation methods under several parameter configurations and operation conditions. The obtained results are analysed and discussed in Section IV. Finally, Section V summarises and concludes the paper.

II. SIGNAL AREA ESTIMATION

A. Problem description and formulation

SA estimation emanates from spectrum measurements, which are based on two-dimensional time/frequency grids. The grids are composed of tiles where every element of the grid corresponds to a single time/frequency tile [8]. When a set of contiguous adjacent tiles are detected as occupied by a signal, a rectangular shaped area is detected, which is referred to as the SA. In this case, the detection distinguishes between two types of tile sets, namely H_0 (not occupied) and H_1 (occupied). The concept of SA refers to a rectangular set of tiles observed in the occupied (H_1) state. The problem of detecting a SA has some similarity to the classical problem of signal detection or spectrum sensing, however there are important differences. First, the focus is not on deciding the instantaneous busy/idle state of a channel but on knowing how spectrum is exploited by its users in order to understand their usage patterns in the time and frequency domains. As a result, an accurate detection of the H_0/H_1 state of every individual tile is in general irrelevant as long as the whole detected SA (i.e., set of tiles) is an accurate representation of the original time/frequency grid actually occupied by the signal (even though some of the individual tiles may be incorrect). Moreover, the detection of H_0/H_1 states in real time is not relevant in SA estimation (as it is in spectrum sensing) since this information is usually not useful in the short term but in the longer term in order to optimise spectrum and radio resource management decisions or, if it is the case,

for spectrum regulatory purposes, network optimisation or any other application scenario where this information may be useful. However, SA estimation methods rely on spectrum sensing decisions and as such are affected by the same two types of errors in the signal detection process, namely missed detections (busy tiles detected as idle) and false alarms (idle tiles detected as busy) [2]. These two errors will affect the particular shapes of the estimated SAs and therefore the performance of the employed SA estimation methods.

The performance of SA is determined by several parameters, which can affect the accuracy and performance. Applying SA will involve sampling the spectrum into a set of observed power levels in the frequency and time domains [8]. The outcome is a set of power levels corresponding to each frequency and time bin or tile in the grid. Then, the power levels are compared to a predefined threshold value, which produces a binary matrix indicating the H_0 or H_1 states of every tile. This binary matrix of busy/idle tiles is the input information provided to the SA estimation method in order to extract the rectangular sets of tiles where one or more SAs are detected in the time/frequency grid. Notice that SA estimation methods are expected to identify perfectly rectangular sets of busy tiles in the time/frequency grid, which can be a challenging task given the corruption introduced by sensing errors in individual tiles.

The process of SA estimation is affected by the employed energy decision threshold as well as the time/frequency resolutions of the data grid. In this case, the resolution in the time domain can be adjusted by modifying the sensing period while the resolution in the frequency domain can be adjusted by modifying the employed FFT size [7]. Therefore, threshold selection and resolution are the main parameters that affect the performance and accuracy of SA techniques and these constitute the focus of this work.

B. Threshold selection methods

The performance of threshold selection can be quantified based on the probability of false alarm (P_{fa}) and the probability of detection (P_d) as shown below [4]:

$$P_d(\lambda) = \mathcal{Q}\left(\frac{\frac{\lambda}{\sigma_w^2} - \mathcal{N}(1 + \gamma)}{\sqrt{\mathcal{N}(1 + \gamma)}}\right) \quad (1)$$

$$P_{fa}(\lambda) = \mathcal{Q}\left(\frac{\frac{\lambda}{\sigma_w^2} - \mathcal{N}}{\sqrt{\mathcal{N}}}\right) \quad (2)$$

where λ represents the threshold, σ_w^2 is the noise power, \mathcal{N} is the number of signal samples, γ is the SNR and $\mathcal{Q}(\cdot)$ is the Gaussian tail probability Q-function [10].

Threshold selection methods that have been studied in [4] including the Constant False Alarm Rate (CFAR), Constant Signal Detection Rate (CSDR), and Minimum Sensing Error Rate (MSER), which are discussed below. These are the most commonly used methods in the literature and ones that will be considered in this work as well.

1) **Constant False Alarm Rate (CFAR)**: The CFAR method is based on a target probability of false alarm value (P_{fa}^*). In this case, equation (2) is solved for the desired false alarm probability to obtain the optimum threshold λ^* as shown below:

$$\lambda^* = \left(Q^{-1}(P_{fa}^*)\sqrt{\mathcal{N}} + \mathcal{N} \right) \sigma_w^2 \quad (3)$$

Notice that this method only requires noise power (σ_w^2) to be estimated in order to calculate the optimum threshold.

2) **Constant Signal Detection Rate (CSDR)**: The CSDR method entails selecting the decision threshold so that a certain target probability of detection (P_d^*) can be attained. In this case, solving (1) leads to the result below:

$$\lambda^* = \left(Q^{-1}(P_d^*)\sqrt{\mathcal{N}} + \mathcal{N} \right) (1 + \gamma) \sigma_w^2 \quad (4)$$

This method requires not only the noise power (σ_w^2) but also the SNR $\gamma = \sigma_x^2/\sigma_w^2$ to be estimated.

3) **Minimum Sensing Error Rate (MSER)**: The MSER method relies on the sensing error function below:

$$P_e(\lambda) = P_{fa}(\lambda) + P_{md}(\lambda) \quad (5)$$

and selects the decision threshold so as to minimise such sensing error function:

$$\lambda^* = \arg \min_{\lambda} P_e(\lambda) \quad (6)$$

Thus, the optimum threshold can be calculated by solving $dP_e(\lambda)/d\lambda = 0$ for λ and is given by:

$$\lambda^* = \left(1 + \sqrt{1 + \frac{2}{\mathcal{N}} \frac{(\gamma + 2)}{\gamma} \ln(1 + \gamma)} \right) \frac{\gamma + 1}{\gamma + 2} \mathcal{N} \sigma_w^2 \quad (7)$$

Thus, the MSER method also requires both SNR and noise power to be estimated in order to calculate the threshold.

C. SA estimation methods

Three different approaches for SA estimation are considered in this work. The first one is a simple tile-by-tile ED, where the individual idle/busy state of each tile in the time/frequency grid is considered. In this case there is no actual estimation of rectangular subsets within the grid associated with any particular SA, in other words, the outcome of the idle/busy decisions of an ED are taken without further processing. This is included in the study simply as a reference benchmark. The CT-SA estimation method proposed in [6] is also considered, where a rectangular SA is estimated based on contour tracing techniques. Finally, the SSA estimation method described in [2], [3], [5] is also included in this study. The latter is a more sophisticated method that estimates every SA present in the time/frequency grid by following several steps. First, a raster scan is performed to find the first corner of a prospective SA. Then, using a unit-width window with height Δt , a horizontal scan is performed to estimate the width of the SA. Afterwards, a coarse estimation of the SA height is carried out with a window with the same width as estimated for the SA and

height ΔT . Finally, a fine height estimation is performed to provide an accurate estimation of the width and height of the SA. The details of this method can be found in [5].

III. METHODOLOGY

A. Simulation procedure

This work adopts a simulation-based evaluation approach. The simulation process aims at testing signal areas under defined transmission constraints. Several random time/frequency test grids are simulated for low, medium and high frequency/time resolutions. These grids include channelized SAs with occupancies randomly generated under well-defined constraints. The generated test grids are then corrupted by adding noise before being fed to the evaluated SA estimation methods, which will operate under different configuration parameters. Finally, the signal area shall be detected based on the three considered methods, namely ED, CT-SA, and SSA. A more detailed description of each simulation step is provided below.

Step 1. Create clean time/frequency test grids: A rectangular time/frequency grid is randomly generated based on a predefined resolution level. The width (number of elements in the horizontal dimension) of the test grid is determined by the considered frequency resolution, while its height (number of elements in the vertical dimension) is determined by the considered time resolution. Three resolution categories are considered, with several resolution levels (in number of tiles for each dimension): low resolution (10×5 , 20×10 and 50×25), medium resolution (100×50 , 200×100 and 500×250), and high resolution (1000×500 , 2000×1000 and 5000×2500). The resolutions of the test grids are specified in the format horizontal \times vertical resolutions in number of tiles.

Channelized signal areas are then generated in the test grid based on specified transmission constraints. In this case, a known number of channels is set in the frequency domain and random on/off transmission durations are generated in the time domain from exponential distributions with rate parameters $\lambda_{on}/\lambda_{off}$ until the total height of the grid is completed for every channel. Furthermore, minimum on/off durations are specified as well as guard bands between channels (i.e., idle tiles in the sides of each channel) as a fraction of the channel width. Fig. 1a shows an example of a randomly generated test grid with five channels, with rate parameters $\lambda_{on}/\lambda_{off} = 0.5$ time units (t.u.), minimum on/off durations of 20 and 10 t.u., respectively, and guard bands of 5% of the channel bandwidth.

Step 2. Add noise to the test grids: Noise is then added to the test grids generated in the previous step. The noise affects both types of tiles (idle and busy). In this process, idle tiles of the test grid may change to busy state with probability P_{fa} while busy tiles may change to idle state with probability $1 - P_d$. The false alarm and missed detection probabilities are calculated according to one of the three considered threshold selection methods described in Section II-B. Fig. 1b shows as an example the test grid of Fig. 1a as detected when the decision threshold is set based on the CFAR method with a target false alarm probability of 10% and SNR of -7 dB.

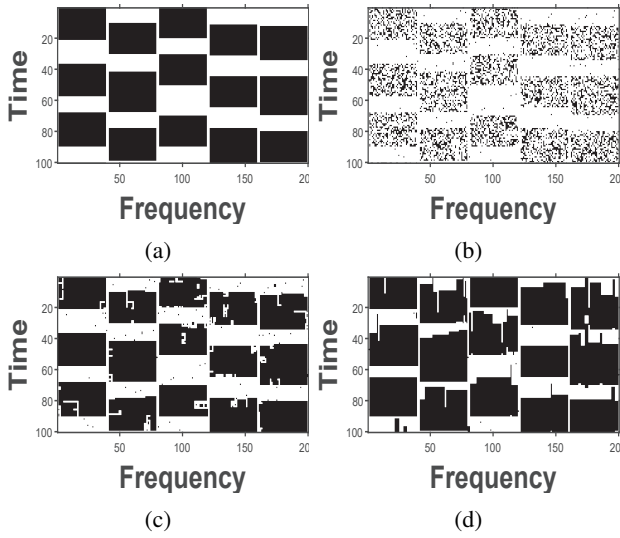


Fig. 1: An example of a randomly generated test grid: (a) Clean time/frequency test grid, (b) Time/frequency test grid with noise, (c) SA estimated by the CT-SA method, (d) SA estimated by the SSA method.

Step 3. Estimate the SA: In this step, one of the SA detection methods described in Section II-C is applied to the noisy test grid in order to estimate the SA present in the original clear test grid. Examples of the SA estimated by CT-SA and SSA methods based on the test grid of Fig. 1b is shown in Figs. 1c and 1d, respectively.

Step 4. Assess the accuracy of the estimated SA: The final step is to assess the accuracy of the estimated SA by comparing the set of SA estimated by the considered method with those present in the original test grid. The accuracy is evaluated based on several performance metrics, which are explained below.

B. Performance Metrics

The probabilities of detection and false alarm are commonly used to assess the performance of signal detection methods. However, these metrics are of little use in the context of SA estimation since the focus is not the accuracy of the detection on every individual tile of the time/frequency signal grid but on the set of SA present, which are the result of some reconstruction processes where subsets of tiles are associated and recognised together as a SA. The analysis of these two probabilities individually does not provide a complete characterisation of the efficacy of the reconstruction implemented in a SA estimation method. Therefore, these probabilities will not be considered individually in this work. Instead, other metrics that take into account the combined impact of these metrics will be considered.

The accuracy of the studied SA estimation methods is assessed in this work by means of two performance metrics. First, a simple Accuracy (ACC) metric is used defined as the percentage of tiles (in either state, idle or busy) that are correctly detected in their real state, which can be obtained

as the sum of true positive and true negative detection rates. In some test grids, the number of tiles in one of the states (idle/busy) may be significantly larger than those in the other state. This motivates the use of the F1 score as our second performance metric, which considers the possible imbalance that may exist between the number of tiles in idle and busy states in the original test grid. The F1 score metric is defined as shown below [11]:

$$F1score = \frac{2 \times TP}{2 \times TP + FP + FN} \quad (8)$$

where TP, FP and FN represent the number of tiles that are a true positive, false positive and false negative, respectively. If the number of idle and busy tiles in the original frequency/time grid are the same, then the F1 score metric reduces to the ACC metric defined above.

The computation time of a SA estimation method will affect the overall performance in a practical system implementation and is therefore evaluated as part of this study as well. Given the existence of a direct correlation between computation time and the overall cost of implementation [7], finding the method that attains the lowest computation time is preferred.

IV. RESULTS

The results obtained for various thresholding and resolution simulations shall be discussed in this section. Simulation results are based on 100 different randomly generated test grids. For the SSA method, the parameters are configured as recommended in [3]. Common simulation parameter setting is shown in Table I.

TABLE I: Simulation parameters

Create clean test grids		Add noise to the test grids		The SSA Method	
number of channels	10	SNR	from -20 dB to 5 dB	Δt	$\min(\min_{on}, \min_{off})$
min_on	width/10	\mathcal{N}	100	ΔT	$\min(\min_{on}, \min_{off}/2)$
min_off	$\min_{on}/2$			γ_{step2}	0.1
λ_{on}	0.05			γ_{step3}	0.15
λ_{off}	0.05				
guard bands	0.05				

A. Impact of the decision threshold

Fig. 2 shows the value of the Accuracy (ACC) metric as a function of the SNR for the considered SA estimation methods (ED, CT-SA and SSA) when different threshold selection methods are employed (CFAR, CSDR and MSER). The results in Fig. 2 were obtained for a grid with a resolution of 100×50 tiles. As it can be appreciated in Fig. 2, the accuracy of the detected SA degrades as the SNR decreases, however several combinations of SA estimation and threshold selection methods show different sensitivity to a reduction in the experienced SNR. The results shown in Fig. 2 indicate that the criterion employed to select the decision threshold has a more significant impact on the resulting accuracy of the estimated SA than the particular SA estimation method itself. As matter of fact, it can be noticed that selecting the decision threshold according to the CSDR method leads to the worst accuracy

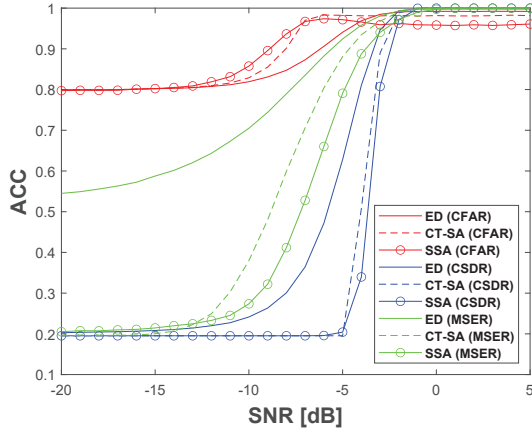


Fig. 2: Accuracy (ACC) as a function of the SNR for the different SA estimation methods (ED, CT-SA, SSA) combined with different threshold selection methods (CFAR, CSDR, MSER).

in the estimated SA, while selecting the threshold according to the CFAR method leads to the best observed accuracy, for all the considered SA estimation methods. The use of different SA estimation methods obviously has an impact on the resulting estimation accuracy, however the criterion used to select the decision threshold has a more significant impact as shown in Fig. 2. This can be explained by the fact that SA estimation methods attempt to detect rectangular SA in the time/frequency grid based on the idle/busy states obtained after applying the selected decision threshold. An inappropriately set decision threshold will lead to a larger number of errors in the detected idle/busy state for each tile in the time/frequency grid and this will make it more difficult for the SA estimation method to correctly identify the existing SAs in the provided grid. Based on the results shown in Fig. 2, it can be concluded that the CFAR method provides the best performance for the three SA estimation methods. Notice that the CFAR method only needs the noise power to be known in order to set the decision threshold (as opposed to the CSDR and MSER methods, which also need the signal power or SNR to be accurately known) and this simplifies the practical implementation in real scenarios. Moreover, it can be noticed that the best accuracy over the whole range of SNR values is in general provided by the SSA method proposed in [5] when the decision threshold is set according to the CFAR method.

Fig. 3 shows the computation time as a function of the SNR for each considered SA estimation method (ED, CT-SA and SSA) and threshold selection method (CFAR, CSDR and MSER)¹. It can be observed that the lowest computation time is for ED, which is the simplest SA estimation method since it does not attempt to reconstruct any rectangular SAs and simply provides the idle/busy state of every tile. Consequently,

¹Notice that the computation time in some cases increases slightly around intermediate values of the SNR. This is because in this region it is more challenging to distinguish clearly the presence/absence of a signal component, thus requiring slightly higher computation times for some methods and configurations.

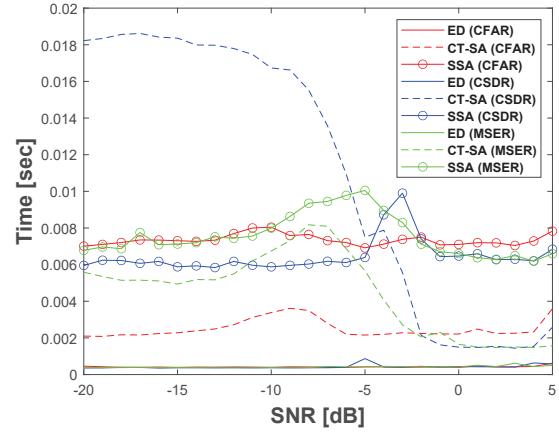


Fig. 3: Computation time as a function of the SNR for the different SA estimation methods (ED, CT-SA, SSA) combined with different threshold selection methods (CFAR, CSDR, MSER).

its computation time is also constant with the SNR since the number of calculations performed by ED (i.e., comparing the power levels to a threshold for each tile) is constant regardless of the experienced SNR. On the other hand, for the CT-SA and SSA methods, the computation times are higher since these methods perform further processing of the tiles in the time/frequency grid in order to reconstruct rectangular SAs. In the case of the CT-SA method, the computation time increases as the SNR decreases as a result of the presence of more errors in the idle/busy states of the tiles at lower SNR, which makes it more difficult to correctly detect the SAs and requires a more computationally expensive processing for the CT-SA method. This is also corroborated by the computation time of the CT-SA method for the different threshold selection methods; notice that the threshold selection methods that provide a better accuracy for the CT-SA method in Fig. 2 also require a lower computation time, since less errors in the idle/busy state of the tiles in the grid means that the CT-SA can reconstruct the SAs not only more accurately (as shown in Fig. 2) but also more efficiently (as shown in Fig. 3). Compared to the ED and CT-SA methods, the SSA method provides an intermediate computation time that shows the interesting property of remaining approximately constant over the whole range of SNR values. This is because the SSA method systematically applies the scanning process described in Section II-C, whose number of calculations does not depend on the presence of errors in the idle/busy state of the tiles in the grid (more errors will decrease the accuracy of the SSA method as shown in Fig. 2 but will not affect the set of computations required by the method, as shown in Fig. 3). This observation for the SSA method is also corroborated by the fact that the computation time of the SSA method is not significantly affected by the criterion used to select the decision threshold as it can be observed in Fig. 3.

Taking into account the results shown in Figs. 2 and 3, the following two observations can be made. When the SNR

is sufficiently high, ED is the preferred approach since it is straightforward to distinguish idle tiles from busy tiles with a very high level of accuracy (even with different values of the decision threshold) and a simple ED approach can provide a (virtually) perfect SA detection (regardless of the employed decision threshold) at the lowest computational cost. When the SNR is moderate to low, the presence of errors in the idle/busy states of the tiles will require some form of more sophisticated processing to detect the SAs and in this case the SSA method provides overall the best trade-off between accuracy and computational cost over the whole range of SNR.

B. Impact of the time/frequency resolution

The analysis presented above showed that the best accuracy for each SA estimation method is obtained when the decision threshold is selected according to the CFAR method. This threshold selection method will be assumed in this section for all the SA estimation methods in order to investigate the impact of the time/frequency resolution on the accuracy of each SA estimation method.

Fig. 4 shows the performance of the accuracy (ACC) metric as a function of the SNR and the frequency/time resolution (in number of tiles for each dimension) of the signal grid. Fig. 5 shows the counterpart of Fig. 4 for the F1 score.

For the ED and CT-SA methods, it can be observed in both figures that the main factor affecting the accuracy of the estimated SA is the SNR. Concretely, as the SNR decreases, the accuracy for the ED and CT-SA methods degrades, as expected, and modifying the time/frequency resolution in these two methods does not have a significant impact on the resulting accuracy. The results shown in Fig. 4 in terms of the ACC parameter suggest that choosing a lower resolution might slightly improve the accuracy, however the improvement observed in Fig. 4 by choosing a lower resolution would be marginal. In the case of the ED and CT-SA methods, where the accuracy remains unaffected by the employed grid resolution, the time/frequency resolution should be decided based on the computational cost and a low resolution may be preferred.

For the SSA method, it can be observed that the accuracy of the estimated SA is affected not only by the SNR but also by the employed grid resolution. A reduction in the experienced SNR will also degrade the accuracy. However, in this case, and in contrast with the ED and CT-SA methods, it is possible to compensate for the degraded detection performance of the SSA method when the SNR decreases by increasing the frequency/time resolution. When a low grid resolution is used with the SSA method, it can be noticed that the SA estimation accuracy will be very close to 100% when the SNR is sufficiently high and will start to degrade when the SNR decreases below about -5 dB. For lower SNR values, it is possible to improve the accuracy by increasing the grid resolution. However, one can use this strategy with the SSA method to a limited extent since simply increasing the grid resolution will not always be able to keep an accuracy close to 100%, in particular if the SNR is very low. Moreover, increasing the resolution beyond certain point will not provide

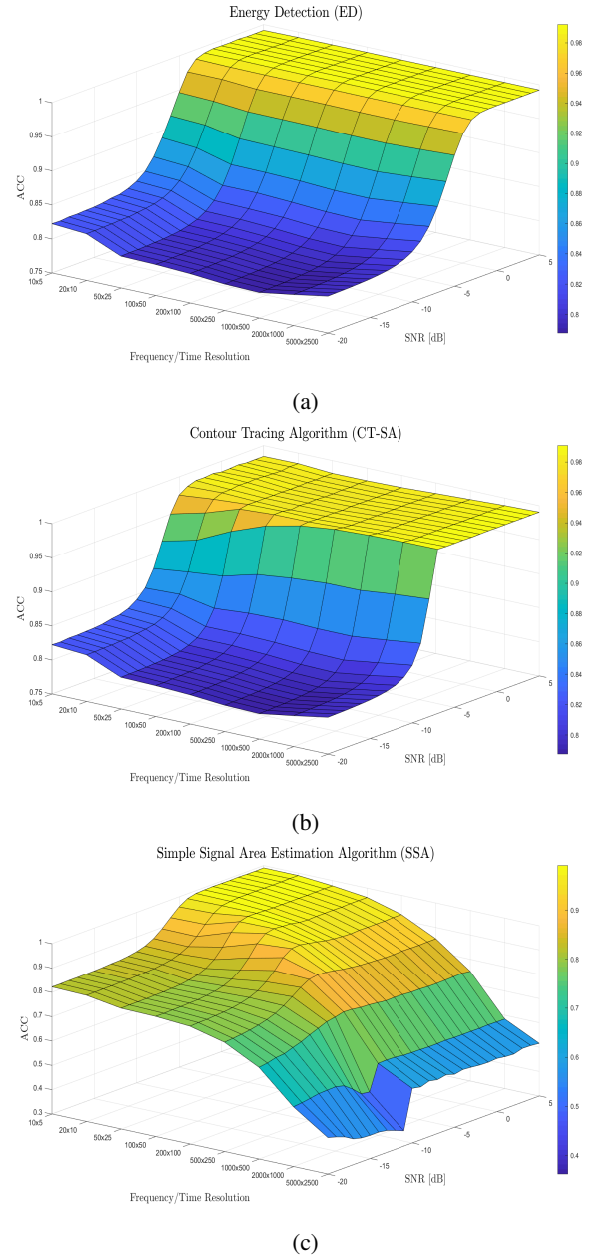


Fig. 4: Accuracy (ACC) as a function of the SNR and the time/frequency resolution for the considered SA estimation methods: (a) ED, (b) CT-SA, and (c) SSA.

an accuracy improvement and, in fact, if the resolution is too high the accuracy of the SSA method will be significantly degraded, even at high SNR (this can be explained by the fact that a higher grid resolution means a higher number of tiles within the same SA and this will increase the probability that the scanning and recognition method used by the SSA method will fall into errors by its own nature). It is interesting to note that, for the SSA method, exists an optimum time/frequency resolution for each SNR value, which provides an additional degree of freedom in the configuration and optimisation of this method compared to the ED and CT-SA methods, where the

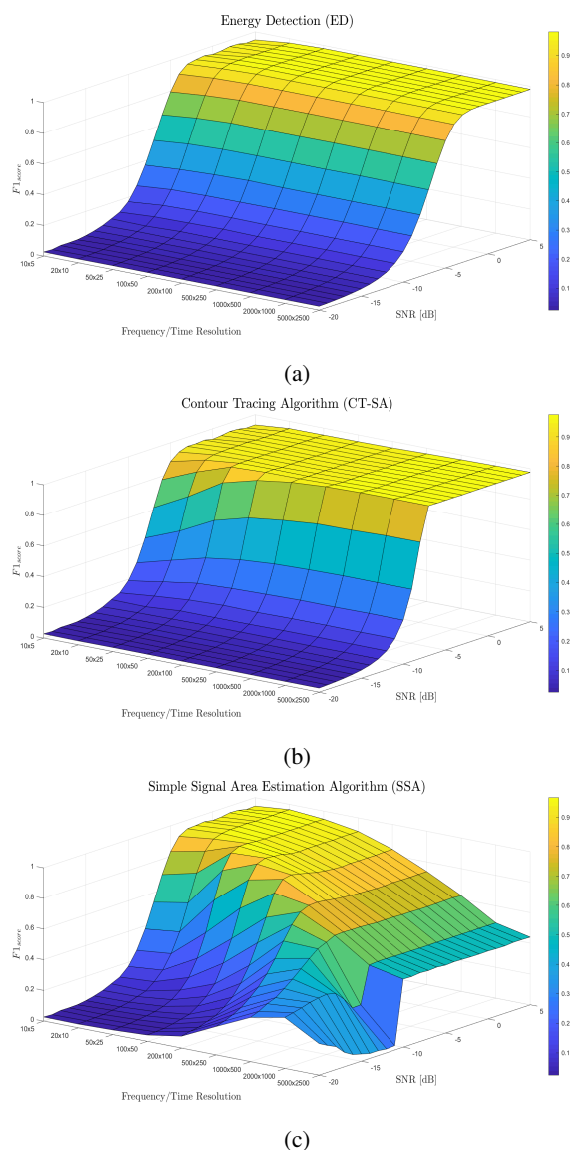


Fig. 5: F1 score as a function of the SNR and the time/frequency resolution for the considered SA estimation methods: (a) ED, (b) CT-SA, and (c) SSA.

variation of the grid resolution has no significant effect.

V. CONCLUSION

This research entailed a comparative study on the impact of thresholding and resolution on SA estimation methods. The investigated SA methods include ED, CT-SA, and SSA. These methods were investigated under threshold selection methods that include CFAR, CSDR and MSER. The performance under different time/frequency resolutions was studied as well. The obtained results indicate that the three considered SA estimation methods achieve their best accuracy when the decision threshold is selected according to the CFAR method (i.e., set for a fixed probability of false alarm), which also has the practical advantage that it only requires the noise power (and not the signal power or SNR) to be known. The best accuracy

over the whole range of SNR values is provided by the SSA method with a decision threshold set based on the CFAR criterion. It has also been observed that the accuracy of the ED and CT-SA methods is mainly affected by the SNR and remains unaffected by the employed grid resolution. However, in the case of the SSA method, the accuracy is also affected by the grid resolution. Interestingly, for the SSA method, a degradation in the accuracy of the estimated SA as a result of a reduced SNR can be compensated (at least to some extent) by selecting the optimum grid resolution for each SNR value, which provides an additional degree of freedom in the configuration and optimisation of the SSA method. Based on the results obtained in this study, the SSA method with a CFAR threshold and an optimum SNR-dependent grid resolution is the preferred approach for SA estimation in spectrum-aware systems and applications.

REFERENCES

- [1] F. Hesar and S. Roy, "Capacity considerations for secondary networks in TV white space," *IEEE Transactions on Mobile Computing*, vol. 14, no. 9, pp. 1780–1793, Sep. 2015.
- [2] R. Mizuchi, K. Umabayashi, J. J. Lehtomaki, and M. López-Benítez, "A study on false alarm cancellation for spectrum usage measurements," in *2017 IEEE Wireless Communications and Networking Conference Workshops (WCNCW)*. IEEE, Mar. 2017, pp. 1–6.
- [3] K. Umabayashi, H. Iwata, J. J. Lehtomäki, and M. López-Benítez, "Study on simple signal area estimation for efficient spectrum measurements," in *2017 European Conference on Networks and Communications (EuCNC)*. IEEE, Jun. 2017, pp. 1–5.
- [4] M. López-Benítez and J. Lehtomäki, "Energy detection based estimation of primary channel occupancy rate in cognitive radio," in *2016 IEEE Wireless Communications and Networking Conference Workshops (WCNCW)*, 2016, pp. 355–360.
- [5] K. Umabayashi, K. Moriwaki, R. Mizuchi, H. Iwata, S. Tiuro, J. J. Lehtomäki, M. Lopez-Benitez, and Y. Suzuki, "Simple primary user signal area estimation for spectrum measurement," *IEICE Transactions on Communications*, vol. 99, no. 2, pp. 523–532, Feb. 2016.
- [6] J. Kokkonen and J. Lehtomäki, "Spectrum occupancy measurements and analysis methods on the 2.45 GHz ISM band," in *2012 7th international ICST conference on cognitive radio oriented wireless networks and communications (CROWNCOM)*. IEEE, Jun. 2012, pp. 285–290.
- [7] R. Mizuchi, K. Umabayashi, J. J. Lehtomaki, and M. López-Benítez, "A study on FFT-ED based signal area estimation for spectrum awareness (short range wireless communications)," *IEICE technical report*, vol. 116, no. 30, pp. 27–34, May 2016. [Online]. Available: <https://ci.nii.ac.jp/naid/40020849217/en/>
- [8] K. Y. Sohn and Y. O. Park, "Method for transmitting and receiving random access channel signal in wireless communication system," Jun. 30 2016, uS Patent App. 14/949,168.
- [9] J. Li, X. Cui, H. Song, Z. Li, and J. Liu, "Threshold selection method for UWB TOA estimation based on wavelet decomposition and kurtosis analysis," *EURASIP Journal on Wireless Communications and Networking*, vol. 2017, no. 1, p. 202, Dec. 2017.
- [10] M. Abramowitz and I. Stegun, *Handbook of Mathematical Functions: With Formulas, Graphs, and Mathematical Tables*, Oct. 1988, vol. 55.
- [11] D. Powers, "Evaluation: From precision, recall and F-measure to ROC, informedness, markedness and correlation," *J. Mach. Learn. Technol*, vol. 2, pp. 2229–3981, Jan. 2011.